6674–6686 Nucleic Acids Research, 2013, Vol. 41, No. 13 Published online 8 May 2013
doi:10.1093/nar/gkt363

Red5 and three nuclear pore components are essential for efficient suppression of specific mRNAs during vegetative growth of fission yeast

Tomoyasu Sugiyama[1,*], Nobuyoshi Wanatabe[2], Eri Kitahata[2], Tokio Tani[2] and Rie Sugioka-Sugiyama[1]

[1]Faculty of Life and Environmental Sciences, University of Tsukuba, Tsukuba, Ibaraki, 305-8577, Japan and [2]Department of Biological Sciences, Faculty of Science, Kumamoto University, Kumamoto, Kumamoto, 860-8555, Japan

Received December 14, 2012; Revised March 29, 2013; Accepted April 16, 2013

ABSTRACT

Zinc-finger domains are found in many nucleic acid-binding proteins in both prokaryotes and eukaryotes. Proteins carrying zinc-finger domains have important roles in various nuclear transactions, including transcription, mRNA processing and mRNA export; however, for many individual zinc-finger proteins in eukaryotes, the exact function of the protein is not fully understood. Here, we report that Red5 is involved in efficient suppression of specific mRNAs during vegetative growth of *Schizosaccharomyces pombe*. Red5, which contains five C3H1-type zinc-finger domains, localizes to the nucleus where it forms discrete dots. A *red5* point mutation, *red5-2*, results in the upregulation of specific meiotic mRNAs in vegetative mutant *red5-2* cells; northern blot data indicated that these meiotic mRNAs in *red5-2* cells have elongated poly(A) tails. RNA-fluorescence *in situ* hybridization results demonstrate that poly(A)$^+$ RNA species accumulate in the nucleolar regions of *red5*-deficient cells. Moreover, Red5 genetically interacts with several mRNA export factors. Unexpectedly, three components of the nuclear pore complex also suppress a specific set of meiotic mRNAs. These results indicate that Red5 function is important to meiotic mRNA degradation; they also suggest possible connections among selective mRNA decay, mRNA export and the nuclear pore complex in vegetative fission yeast.

INTRODUCTION

A zinc-binding domain was first discovered within the DNA-binding domain of TFIIIA; since then, closely related zinc-binding domains, which are found in many eukaryote proteins, have been studied intensively (1). These zinc-binding domains are classified into two types, 'classical' and 'novel' zinc-finger domains. 'Classical' zinc-fingers bind nucleic acids and have important roles in various transactions, such as transcription, mRNA processing and mRNA export (1). 'Novel' zinc-fingers—ZnF UBP, GATA, LIM, RING and PHD—act as protein-interaction domains: PHD binds Lys^4-trimethylated histone H3, and ZnF UBP binds to ubiquitin (1). Novel zinc-finger proteins are implicated in ubiquitin-dependent proteolysis, chromatin regulation and hypoxic responses, as well as transcriptional regulation (1). Moreover, with recently developed artificial zinc-finger-nucleases, researchers can manipulate specific sites within the genomes of higher eukaryotes, such as mice and zebrafish (2). Numerous zinc-finger proteins have been studied: nonetheless, the function of many individual genes that encode a zinc-binding domain is largely unknown because such genes are common in eukaryotes.

The fission yeast *Schizosaccharomyces pombe* is an excellent model organism with which to study sexual differentiation, that is, meiosis (3). Previous studies demonstrates that expression of numerous meiotic genes is transcriptionally regulated (4,5). However, at least some of meiosis-specific genes, such as *mei4*$^+$ and *crs1*$^+$, are transcribed both in mitosis and in meiosis, but these meiotic mRNAs are rapidly degraded to prevent the ectopic expression of these meiotic mRNAs in vegetative cells (6–8). The system responsible for this mRNA degradation depends on mRNA degradation sequences (UUAA

*To whom correspondence should be addressed. Tel: +81 29 853 7323; Fax: +81 29 853 7322; Email: sugiyamt@tara.tsukuba.ac.jp
Present address:
Tomoyasu Sugiyama, Life Science Center of Tsukuba Advanced Research Alliance, University of Tsukuba, 1-1-1 Tennodai, Tsukuba, 305-8577, Japan.

AC/UCAAAC) called determinant of selective removal (DSR) in the targeted meiotic mRNAs, an RNA-binding protein Mmi1, polyadenylation factors, a nuclear poly(A)-binding protein Pab2, a CCCH-type zinc-finger protein Red1 and the nuclear exosome (6,8–12). However, the detailed mechanism by which the mRNA decay system specifically activates nuclear exosome-mediated mRNA degradation is currently unknown, and additional, yet-identified, factors probably function in this system.

Nuclear pore complexes (NPCs) are large (~60–125 MDa in mammals and ~40–60 MDa in yeasts) structures comprising ~30 core nucleoporin proteins (Nups) and many accessory proteins (13,14). The NPCs mediate nucleocytoplasmic transport in eukaryotes; they are freely permeable to small molecules, including metabolites and ions, but they act as molecular sieves for macromolecules, such as proteins and ribonucleoproteins (13,14). In addition to their roles in nuclear import and export, the NPCs play important roles in gene expression: (i) *Saccharomyces cerevisiae* Nup2 is necessary and sufficient to create boundary elements that divide euchromatin from heterochromatin when Nup2 is tethered to DNA directly; (ii) the NPC-associated Spt-Ada-Gcn5 acetyltransferase (SAGA) chromatin remodeling complex recruits the promoters of inducible genes to promote their transcription; and (iii) Trf4-Air2-Mtr4 polyadenylation (TRAMP) complex and other surveillance factors with the nuclear exosome apparently retain or degrade aberrant or non-functional RNA species in the vicinity of the NPCs (13,15,16). Moreover, changes in NPC composition have been recently shown to regulate cell differentiation, and mutations in *NUP155* and *NUP62* cause atrial fibrillation and infantile striatal necrosis, respectively, in humans (17–19). These findings strongly suggest that the NPC provides a platform for regulating gene expression at both transcriptional and post-transcriptional levels, and that each component of the NPCs may have a specific role in development and differentiation.

Using a localization-based approach, we have identified several factors that localize to nuclear foci in fission yeast, and we found that two such nuclear proteins, Red1 and Rhn1, are essential factors for suppressing meiotic mRNAs in vegetative fission yeast (11,20). Here, we demonstrate that Red5, a previously uncharacterized protein that localizes as nuclear dots, is essential for the selective elimination of DSR-containing meiotic mRNAs in vegetative *S. pombe*. In addition, our data indicate that mRNA degradation and NPCs are functionally connected. The identification and characterization of Red5 should help to further elucidate the detailed mechanism of meiotic mRNA decay in fission yeast.

MATERIALS AND METHODS

Strains, media and plasmids

The general genetic methods used in this study were described previously (21). Complete medium (YEA), minimal medium (PMG), PMG without uracil (PMG-ura), PMG lacking leucine (PMG-leu) and nitrogen-free PMG (PMG-N) were used to culture the cells (21,22). Strains expressing tdTomato, mCherry (23), GFP (24), FLAG, myc or PK epitope-tagged proteins, deletion strains and the C-terminal truncated Red5 (1–331) strain (Red5ΔC-GFP) were constructed using polymerase chain reaction (PCR)-based methods as described previously (25). The C-terminal GFP tag on Uap56 did not affect viability, but it resulted in a slight growth retardation. We then named the *uap56*$^+$-GFP allele *uap56-1*.

Random mutagenesis of *red5*$^+$ was performed essentially as described previously (26). Briefly, we obtained 103 of G418-resistant colonies, and we subjected each clone to a temperature-sensitivity test by incubating replicated plates at 26 or 37°C. Of the 103 clones, 23 were selected because they apparently grew slowly at 37°C; these 23 clones were then subjected to dilution analysis to test again for temperature sensitivity. Of these 23 clones, one (#2) formed smaller colonies than wild-type cells when grown at 34°C, and this clone (hereafter *red5-2*) was further examined via western blotting and genomic sequencing. The *red5-2* strain carried three mutations in the *red5*$^+$ coding region, but only one of these mutations (T701C) resulted in an amino acid substitution (I234Y). All the strains used in this study are listed in Supplementary Table S1.

To express Red5, Mmi1 or HA-tagged Rae1 in fission yeast, REP3X-*red5*$^+$, REP41X-*red5*$^+$, REP1-*mmi1*$^+$ or REP41HA-*rae1*$^+$ constructs were used.

Microscopy

An Axio Imager M1 microscope (Carl Zeiss MicroImaging) was used for differential interference contrast and fluorescent microscopy. The raw images were processed using AxioVision software (Carl Zeiss MicroImaging). For RNA-fluorescence *in situ* hybridization (FISH), an Olympus AX70 fluorescence microscope equipped with a Photometrics Quantix cooled CCD camera or a Nikon Eclipse Ti-E inverted microscope with a Hamamatsu ORCA-R2 cooled CCD camera was used to examine hybridized cells, and IPLab (Scanalytics, Inc.) or MetaMorph software (Molecular Devices) was used to collect digital images. Selective contrast enhancement was not applied to the RNA-FISH images.

Serial dilution analysis

Dilution analyses were performed as described previously (27). Briefly, 10-fold serial dilutions of exponentially proliferating cultures were spotted on YEA plates, or on YEA plates with 15 μg/ml thiabendazole, 10 mM hydroxyurea or 2 mU/ml bleomycin. For analysis of ultraviolet (UV) sensitivity, YEA plates spotted with serial dilutions were exposed to 180 J/m^2 of ultraviolet using a UV cross-linker (UVP); these plates were then incubated for 3–5 days at 30°C unless otherwise specified. To test for genetic interaction, 10-fold serial dilutions of exponentially growing cultures were spotted on YEA plates and then incubated for 3–7 days at indicated temperatures. For Red5 or Mmi1 overexpression, each strain carrying a REP plasmid was washed with water four times to remove thiamine. Samples from the 10-fold serial dilutions of each strain were spotted on leucine-deficient minimal

plates (PMG-Leu) with or without 5 μg/ml thiamine and incubated at 26, 30 or 32°C for 3 –4 days.

Immunoprecipitation and western blotting

Immunoprecipitation experiments were performed as described previously (28). Briefly, cell lysates from exponentially growing fission yeast strains expressing tagged proteins were incubated with anti-DDDDK (PM020, MBL), anti-HA (561, MBL), anti-V5 (PM003, MBL) or anti-GFP (RQ2, MBL) antibody. Immunoprotein complexes were recovered by incubation with protein A/G magnetic beads (Life Technologies) and were then subjected to western blotting using anti-c-Myc (A-14, Santa Cruz, or 9E10, Covance), anti-GFP (7.1 and 13.1, Roche Applied Science), anti-V5 (V5005, Nacalai Tesque) or anti-FLAG antibody (M2, Sigma) as probes.

RNA analyses

Preparation of RNA samples from vegetatively growing fission yeast cells in complete or minimal media was performed as described previously (11). For RNA isolation from temperature-sensitive mutant strains (*red5-2*, *rae1-167*, *ptr1-1* or *mog1-1*), each strain was cultured at 26°C, then shifted to 37°C and cultured at 37°C for 4 h before cells were harvested. RNA samples were collected and then subjected to reverse transcriptase (RT)–PCR or northern blot analysis; the RT–PCR was performed with the PrimeScript® II first strand cDNA synthesis kit (TaKaRa Bio Inc.) and *TaKaRa ExTaq*® (TaKaRa Bio Inc.); the northern blot analysis was performed with 5′-digoxigenin (DIG)-labeled oligonucleotide probes (70mer), DIG Easy Hyb (Roche Applied Science), anti-DIG Fab fragment conjugated with alkaline phosphatase (Roche Applied Science), the DIG Wash and Block Buffer set (Roche Applied Science) and CDP-Star™ (GE Healthcare). To assess whether $rec8^+$ or $spo5^+$ mRNAs were hyperadenylated in *red5-2* cells, DNase-treated total RNA samples were incubated with RNase H (New England Biolabs Inc.) in the presence or absence of oligo $(dT)_{15}$ primer (TaKaRa Bio Inc.) and were then subjected to northern blot analysis.

For microarray analyses, the *S. pombe* expression 4 × 72 K array (090408 Spom exp X4, Roche Applied Science) was used; microarray analyses were performed according to the manufacturer's protocol. The data from wild-type cells were compared with those from *red5-2* cells; the transcripts that showed >2-fold increase or <0.5-fold decrease were selected as 'increased' or 'decreased' mRNAs, respectively. The increased or decreased genes are listed in Supplementary Tables S2 and S3, respectively. The statistical significance (*p*-value) of the overlap of two groups (genes changed in *red5-2* cells versus in *red1*Δ cells) was determined by hypergeometric probability distribution using a calculation program (http://nemates.org/MA/progs/overlap_stats.html). The microarray data can be accessed at NCBI GEO under the accession number GSE44714.

The intracellular distribution of poly(A)$^+$ RNAs in *S. pombe* was determined by FISH with a biotin-labeled oligo dT (50mer) probe as described previously (29).

RESULTS

Red5 is a novel zinc-finger protein that forms nuclear dots

To identify novel factors that form nuclear dots in fission yeast, we examined the localization of fluorescently tagged versions of uncharacterized proteins. We previously reported that two such proteins, Red1 and Rhn1, are involved in meiotic mRNA suppression in vegetative *S. pombe* (11,20). In addition to these two proteins, we found that a previously uncharacterized protein (SPBC337.12) fused with a GFP tag at its C-terminus localized to 1–3 discrete dots in the nucleus (Figure 1); we named this protein Red5 (RNA elimination defective 5). To further examine where the Red5 dots localized, we compared the localization of Red5 with that of Hta1, an H2A histone. Weak Red5 signal was evenly distributed in regions of chromatin that contained Hta1; additionally, Red5 foci were often found at the edges of chromatic domains (Figure 1, top). Because non-chromatic domains of *S. pombe* nuclei are equivalent to the nucleoli of higher eukaryotes, we compared the localization of Red5 with that of a nucleolar protein Gar2, which is homologous to Nucleolin (30). Interestingly, Red5 foci were present both in and at the edges of Gar2-positive domains (Figure 1, bottom). These results indicated that Red5 is uniformly distributed in chromatic domains, and Red5 dots are often found in the nucleolus and apparently at the boundaries between chromatin and nucleoli.

Red5 was predicted to be a 376-amino acid protein that has five C3H1-type zinc-finger domains in tandem (Supplementary Figure S1A). A BLAST search indicated that Red5 has homology to the ZC3H3 proteins in various eukaryotic species, including human, mouse, rat, chicken and fly (Supplementary Figure S1B); however, this homology was limited to the zinc-finger domains (Supplementary Figure S1C). Additionally, the zinc-finger domains of Red5 resemble the YTH1 domain (Supplementary Figure S1D) found in Yth1, an mRNA

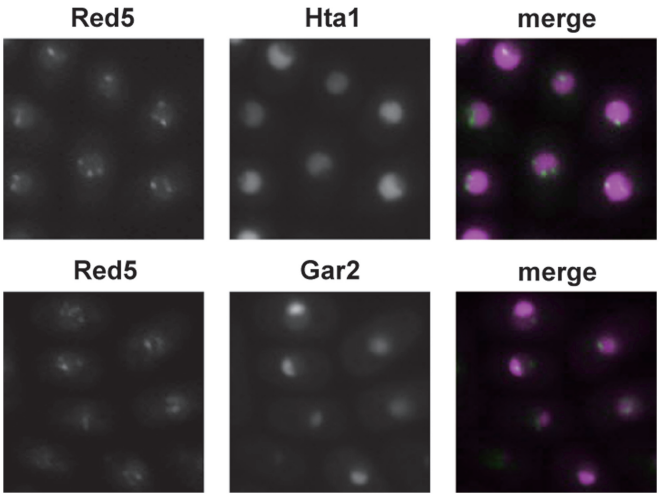

Figure 1. Red5 forms nuclear foci. Vegetative fission yeast cells expressing Red5-GFP (Red5) and Hta1-mCherry (Hta1) (top) or Red5-GFP and Gar2-mCherry (Gar2) (bottom) were analyzed using a fluorescence microscope. Representative images are shown.

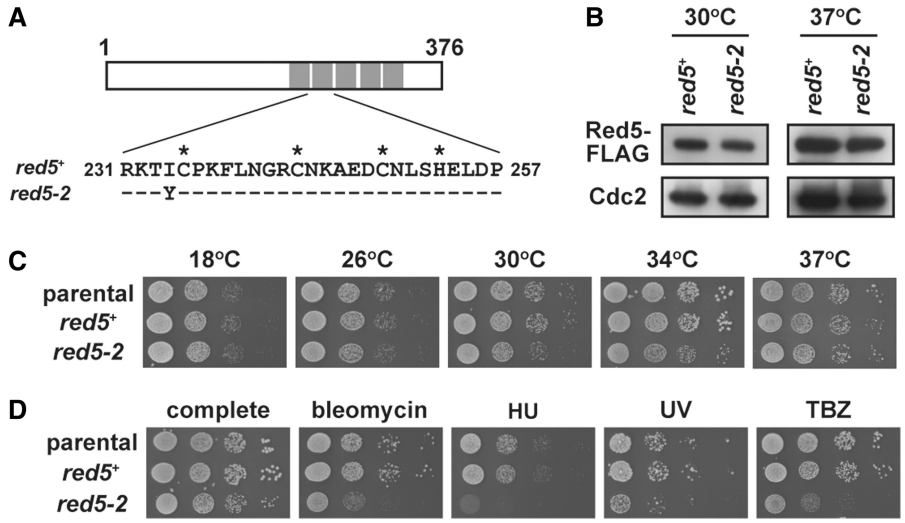

Figure 2. *red5-2* cells are hypersensitive to various stresses. (**A**) *red5-2* cells have an Ile^{234} to Tyr substitution. The asterisks indicate the conserved residues of the second CCCH-type zinc-finger domains. (**B**) The I234Y mutation does not affect the abundance of Red5. Protein extracts from Red5–FLAG (*red5*$^+$) and $Red5^{I234Y}$–FLAG (*red5-2*) strains were examined on western blots probed with anti-FLAG or anti-Cdc2 antibody. Cdc2 was monitored as a loading control. (**C** and **D**) Serial dilutions of parental wild-type (parental), *red5*$^+$–FLAG (*red5*$^+$) and $red5^{I234Y}$–FLAG (*red5-2*) cultures were spotted onto YEA plates (C) or were spotted onto YEA plates (complete) and YEA plates supplemented with 2 mU/ml bleomycin, 10 mM hydroxyurea (HU) or 15 μg/ml TBZ (D). For UV treatment, spotted plates were exposed to 180 J/m^2 of UV. The plates were then incubated at the indicated temperatures (C) or at 30°C (D).

cleavage and polyadenylation specificity factor (31). A previous study showed that human and *Drosophila* ZC3H3 proteins have an important role in both polyadenylation and export of mRNAs (32). These results indicate that Red5, or at least the zinc-finger domains found in Red5, is conserved among eukaryotes, and that Red5, like ZC3H3 proteins, could regulate RNA metabolism through its zinc-finger domains.

red5-2 cells are sensitive to DNA damaging and microtubule-destabilizing agents

To investigate Red5 function, we attempted to construct a strain carrying a loss-of-function mutation in *red5*$^+$ because a previous study showed that *red5*$^+$ is one of the genes that is essential for cell viability (33). We used a PCR-based method to randomly mutate *red5*$^+$, and we isolated the *red5-2* (SP1479) strain (see 'Materials and Methods' section). We sequenced the *red5*$^+$ coding region from the *red5-2* cells and found that *red5-2* cells carried a single amino acid substitution, Ile^{234} to Tyr^{234} (I234Y), between the first and the second zinc-finger domains (Figure 2A). As Ile^{234} is right next to Cys^{235}, which is a conserved residue that holds the Zn^{2+} ion in the second zinc-finger domain, the amino acid change might affect the affinity for Zn^{2+} ion. Western blot data indicated that $Red5^{I234Y}$–FLAG was almost as abundant as Red5–FLAG at both 30 and 37°C (Figure 2B), indicating that the I234Y substitution did not alter the steady-state level of Red5 protein.

We then tested temperature sensitivity of *red5-2* cells and found that at 30 and 34°C, *red5-2* cells formed smaller colonies than did parental (FY12806) or *red5*$^+$–FLAG (SP1428, hereafter *red5*$^+$) cells; we did not observe obvious growth differences among the three strains at 37°C, a temperature at which fission yeast cells grow more slowly than they do at 30 or 34°C (Figure 2C). To further confirm the growth retardation of *red5-2* cells at 34°C, we compared growth curves of liquid-cultured *red5*$^+$ cells at 34°C with *red5-2* cells at 34°C. We found that at 34°C, *red5-2* cells grew more slowly than *red5*$^+$ cells did (Supplementary Figure S2). These results showed that the *red5-2* mutation weakly affected growth rate.

Mutations in any of several RNA-binding or zinc-finger proteins cause growth defects in fission yeast subject to stress such as DNA damage or genomic instability (34–38). Because Red5 is a putative RNA-binding protein, we hypothesized that *red5-2* might display higher sensitivity to genotoxic stresses. To test this hypothesis, we assessed the growth of *red5-2* cells that were exposed to DNA damage or thiabendazole (TBZ), a microtubule-destabilizing agent. As shown in Figure 2D, *red5-2* was more sensitive to bleomycin, hydroxyurea, UV and TBZ than control cells were. These results indicated that Red5 could be involved in a stress response pathway and in the maintenance of genomic stability.

Red5 is required for efficient mating and sporulation

Several RNA-binding proteins, including Mei2, Spo5 and Meu5, have been implicated in meiosis in fission yeast (39–41). When meiosis was induced in three homothallic strains—parental (FY12806), *red5*$^+$ (SP1428) and *red5-2* (SP1479)—by nitrogen depletion, we found that *red5-2* cells hardly mated and produced fewer asci compared with parental or *red5*$^+$ cells (Figure 3A, left). Consistent with this result, parental and *red5*$^+$, but not *red5-2*, colonies showed dark staining patterns after exposure to iodine vapor, which labels asci (Figure 3A, right). The mating efficiency of these strains was 65.9% (wild-type),

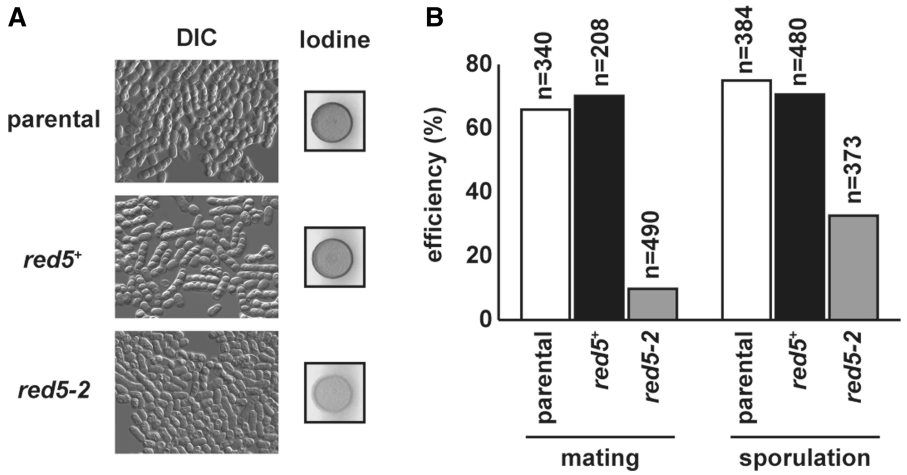

Figure 3. The *red5-2* mutation affects meiosis. (**A**) Cells from each homothallic culture—parental wild-type (parental), *red5*$^{+}$–FLAG (*red5*$^{+}$) or *red5*^{I234Y}–FLAG (*red5-2*)—were spotted onto PMG plates and incubated at 26°C for 3 days. The presence or absence of tetrads was confirmed by differential interference contrast (DIC) imaging (left) and by iodine staining (right). (**B**) The mating and sporulation efficiencies of parental wild-type (parental), *red5*$^{+}$–FLAG (*red5*$^{+}$) and *red5*^{I234Y}–FLAG (*red5-2*) cells; 'n' indicates the number of cells counted in each strain.

70.2% (*red5*$^{+}$) and 9.8% (*red5-2*) (Figure 3B). We also assessed sporulation efficiency of diploid *red5-2* cells (SP1989) and found that sporulation in *red5-2* cells was relatively inefficient (32.7%) compared with parental (SP1987; 75%) and *red5*$^{+}$ (SP2010; 70.6%) cells (Figure 3B). These results demonstrated that Red5 facilitates both mating and sporulation.

The levels of meiotic mRNAs increase in *red5*-deficient cells

We next performed mRNA profiling of vegetative *red5-2* cells to identify genes affected by the *red5* mutation. In a microarray analysis, we identified 47 mRNAs that were upregulated >2-fold in vegetative *red5-2* relative to wild-type cells. The majority of these mRNAs, 43/47 (91.5%), were previously reported to be induced during nitrogen starvation or meiosis (4,5) (Figure 4A; Supplementary Table S2). Among the 47 mRNAs, two (4.25%) were non-meiotic mRNAs, and another two mRNAs (4.25%) are not known to be meiosis related (Figure 4A; Supplementary Table S2). We also identified 20 mRNAs with steady-state levels that were lower (<0.5-fold reduction) in *red5-2* than in wild-type cells (Figure 4B; Supplementary Table S3). Most of these downregulated genes, 17 of 20 (85%), were located in subtelomeric regions (Supplementary Figure S3A), and 7 of the 20 decreased mRNAs (30%) were classified as meiotic genes (Supplementary Table S3). We performed RT–PCR experiments to confirm some of these array results (Supplementary Figures S3B and C). These results demonstrated that Red5 has two roles in vegetatively growing cells: (i) to suppress meiotic mRNAs and (ii) to maintain expression of several genes, in particular, genes located at subtelomeric domains.

Red5 is required for DSR-mediated mRNA decay

Many meiotic mRNAs—*mei4*$^{+}$, *rec8*$^{+}$, *ssm4*$^{+}$ and *spo5*$^{+}$—are transcribed both in mitosis and in meiosis, and these mRNAs are degraded by DSR (determinant of selective removal)-dependent mRNA decay (42). Given that Red5 negatively regulated DSR-containing mRNAs, it was plausible that Red5 participated in this pathway for the elimination of meiosis-specific transcripts in vegetative cells. To test this hypothesis, we compared the Red5-regulated genes (genes that were upregulated or downregulated in *red5-2* cells relative to wild-type cells) with Red1-regulated genes (11); we found that the set of Red5-regulated genes overlapped with that of Red1-regulated genes. Specifically, 39 of 47 mRNAs (83%) upregulated in *red5-2* cells were also upregulated in *red1*Δ cells ($p < 7.7\times10^{-58}$) (Figure 4C), whereas 9 of 20 mRNAs (45%) downregulated in *red5-2* cells were also downregulated in *red1*Δ cells ($p < 4.5\times10^{-16}$) (Figure 4D). These results indicated that Red5 and Red1 suppress or promote the expression of common target mRNAs in vegetative cells, and that the two proteins are closely related in function.

Our analyses indicated that Red5 promoted the selective elimination of DSR-containing meiotic mRNAs; however, it remained unclear whether Red5, like Red1 and Mmi1, is essential for the DSR-mediated mRNA elimination. To address this issue, we generated wild-type and *red5-2* mutant strains that each carried a *ura4*$^{+}$-DSR marker (Figure 5A, top) and then examined whether the *red5-2* mutation affected degradation of the *ura4*$^{+}$-DSR mRNA. RT–PCR results indicated that *ura4*$^{+}$-DSR mRNA accumulated in *red5-2* and in *red1*Δ cells, but not in wild-type cells (Figure 5A, bottom). From these data, we concluded that Red5 cooperates with other protein factors, such as Mmi1 and Red1, to exert DSR-directed degradation of meiotic mRNAs in vegetative cells.

In cells lacking Rrp6, which is a cofactor of the nuclear exosome, meiotic mRNAs, such as *rec8*$^{+}$ and *spo5*$^{+}$ mRNAs, have highly elongated poly(A) tails, but not in *red1*Δ, *mmi1*- or *pla1*-deficient cells (8,9,11); the hyperadenylation seen in Rrp6-deficient cells is proposed to be prerequisite for degradation by the nuclear exosome (8,9). Therefore, we determined which

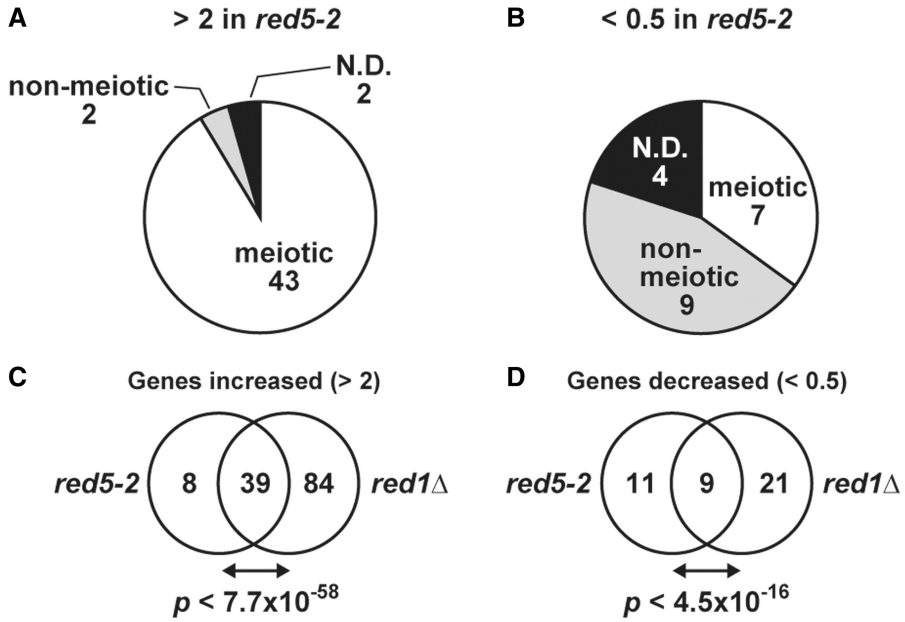

Figure 4. Red5 is essential for selective removal of meiotic mRNAs in vegetative cells. (**A**) A large fraction of the mRNAs that accumulated in growing *red5-2* were meiotic mRNAs. Expression analyses with a microarray technique demonstrate that 91% of increased (>2-fold) transcripts in *red5-2* cells have previously been reported as genes upregulated in response to nitrogen starvation, pheromone treatment or during meiosis. (**B**) Transcripts decreased (<0.5) in vegetatively growing *red5-2* cells; these genes were classified as meiotic, non-meiotic or not determined (N.D.) according to a previous study (4). (**C** and **D**) The numbers of genes that had increased >2-fold (C) or decreased <0.5-fold (D) expression in the *red5-2* cells or *red1*Δ cells are presented in Venn diagrams. For each comparison, the same set of 4977 genes was examined. Statistical significance (*p*-value) of the overlap between each of the two groups is shown under each diagram.

step, hyperadenylation or mRNA degradation, was affected in *red5-2* cells. Northern blot data demonstrated that *red5-2* cells, like *rrp6*Δ cells, were characterized by hyperadenylation of $rec8^+$ and $spo5^+$ mRNAs, and this pattern was not evident in *red1*Δ or *red5-2 red1*Δ double-mutant cells (Figure 5B). In addition, the smeary signals from $rec8^+$ and $spo5^+$ mRNAs were abolished when RNA samples were treated with RNase H in the presence of oligo(dT) primer (Figure 5C). These results indicated that Red5 function was dispensable for meiotic mRNA hyperadenylation directed by Red1/Mmi1/Pla1, and suggested that Red5, like Rrp6, worked at one or more steps that are a downstream of hyperadenylation of meiotic mRNAs. Currently, we recognize the possibility that Red5 promotes target mRNA degradation by helping the nuclear exosome to find and/or to degrade its hyperadenylated mRNA substrates.

The *red5-2* mutation suppresses the sporulation deficiency of *sme2*Δ cells

Inactivation of the Mmi1-DSR system rescues a meiotic defect of *sme2*Δ (6,9,10). As Red5 is involved in DSR-dependent mRNA decay, we expected that *red5-2* might suppress the *sme2*Δ meiotic phenotype. To test this hypothesis, we combined *red5-2* mutation with the *sme2* deletion and examined whether *red5-2 sme2*Δ cells formed spores more efficiently than *sme2*Δ cells did. Homothallic *sme2*Δ cells mated and became diploid cells efficiently, but they did not sporulate efficiently (1.4%); in contrast, homothallic *red5-2 sme2*Δ cells sporulated efficiently (61.4%, Supplementary Figure S4). These results demonstrated that the *red5-2* mutation suppresses the meiotic defect caused by *sme2*Δ, and further support the notion that Red5 plays an important role in selective elimination of meiotic mRNAs.

Red5 colocalizes with Red1, Mmi1 and Pab2 in mitotic cells

Red5 and Red1 share target mRNAs; therefore, we speculated that Red5 may colocalize and associate with proteins involved in DSR-dependent mRNA decay. To test this hypothesis, we investigated whether Red5 colocalized with Red1, Mmi1 and Pab2. Specifically, sequences encoding fluorescent protein tags were fused in-frame to the genomic loci that encode each endogenous protein, and the localization of each fluorescently tagged fusion proteins, which were expressed from the respective endogenous genomic loci, was assessed. As we anticipated, Red5 colocalized with Red1, Mmi1 and Pab2 in mitotically dividing cells (Supplementary Figure S5A). We next performed a series of immunoprecipitation assays to assess potential physical interaction between Red5 and several proteins, including Red1 and Mmi1. We found that Red5 was coimmunoprecipitated with Pab2; however, it seemed that only a small fraction of Red5 immunoprecipitated with Pab2 (Supplementary Figure S5B). Conversely, Red5 was not coimmunoprecipitation with Red1, Mmi1, Pla1, Rrp6 or the 3′-processing factors—Pfs2, Rna15, Pcf11, Mpe1 (SPBP8B7.15c, homologous to *S. cerevisiae* Mpe1), Cft1 and Msi2 (SPBC660.15, homologous to *S. cerevisiae* Hrp1) (Supplementary Figures S5C–E). Because Red1 interacted

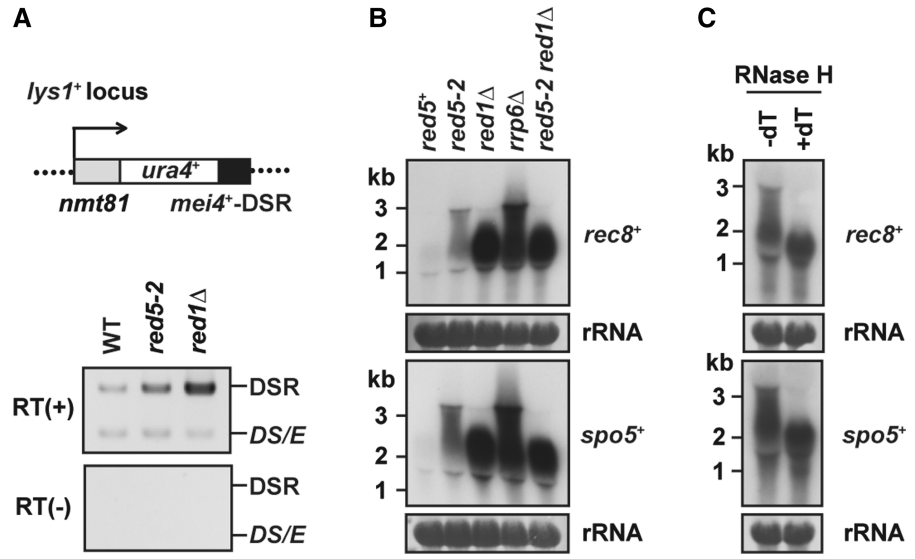

Figure 5. Red5 promotes DSR-directed mRNA degradation after polyadenylation of target mRNAs. (**A**) Red5 is required for DSR-dependent mRNA decay. (top) Schematic representation of the *ura4*$^+$-DSR construct. This construct consists of the DSR region derived from *mei4*$^+$ and the open reading frame from *ura4*$^+$; *ura4*$^+$-DSR transcription is driven by the *nmt81* promoter. (bottom) Wild-type (WT), *red5-2* or *red1*Δ cells carrying both the *ura4*$^+$-DSR (DSR) and a *ura4*$^+$ minigene (*ura4DS/E*, *DS/E*) were grown in the absence of thiamine and then subjected to RT–PCR. The *ura4DS/E* was used as the internal control. (**B**) Meiotic mRNAs in *red5-2* cells are elongated. Northern blotting was performed to analyze *rec8*$^+$ and *spo5*$^+$ mRNAs in *red5*$^+$, *red5-2*, *red1*Δ, *rrp6*Δ or *red5-2 red1*Δ cells. The same blots were stained with methylene blue to visualize 28S ribosomal RNAs (rRNA), which serve as the loading control. (**C**) The elongation of *rec8*$^+$ and *spo5*$^+$ mRNAs results from excessive polyadenylation. RNA samples from *red5-2* cells were treated with RNase H in the presence (+dT) or absence (−dT) of oligo(dT)$_{15}$ primer and then were analyzed on northern blotts. The 28S ribosomal RNAs (rRNA) stained with methylene blue serve as the loading control.

with Mmi1, Pla1 and Rrp6, but not with Pab2 in our hands (11), Red5-Pab2 and Red1-Mmi1-Pla1-Rrp6 heteromers could be constituents of distinct subcomplexes or interact weakly or transiently, although they colocalize. In addition, a previous study demonstrated that dZC3H3 associates with PABPN1 in flies (32); therefore, the interaction between ZC3H3 proteins and nuclear poly(A)-binding proteins may be conserved in fission yeast and fly.

Red5 foci disappear in response to the activation of pheromone signaling

Red1 and Mmi1 have different localization patterns in meiotic cells; Mmi1 starts to converge into a dot at the conjugation stage, and the Mmi1 dot disperses into multiple nuclear foci after meiosis I, whereas Red1 foci disappear on the activation of pheromone signaling and they re-appear after meiotic chromosome segregation is completed (6,11). We examined whether Red5 localization is altered on the initiation of meiosis. To do this, we used an h^- strain that carries a *matPc* construct (strain designation h^- *lys1*$^+$::*matPc*). Because of Pc expression from the *lys1*$^+$::*matPc* construct, nitrogen deprivation leads to activation of pheromone signaling even in h^- cells (43). As we described previously, Red1 signals were gradually lost in h^- *lys1*$^+$::*matPc* cells when the nitrogen source was eliminated (Supplementary Figure S6, middle). Notably, Red5 dots were lost more quickly than were Red1 dots; specifically, Red5 dots persisted only 1.5 h after the onset of nitrogen deprivation, whereas Red1 dots did 4.5 h. However, diffuse, rather than concentrated, Red5 signal persisted in the nucleoplasm, but seemed to decrease gradually (Supplementary Figure S6, bottom). These results clearly demonstrated that activation of pheromone signaling elicits the disassembly of Red5 dots and that localization patterns of Red5, Red1 and Mmi1 are each regulated differently during the initiation of meiosis.

The C-terminal domain of Red5 is required for normal cell growth, mating and meiotic mRNA elimination, but not for the formation of Red5 foci

To further characterize the Red5 protein, we constructed a strain that lacked distinct C-terminal regions of Red5 (amino acid number 332–376, henceforth Red5ΔC; Figure 6A). Western blot data demonstrated that the protein level of Red5ΔC-GFP was as abundant as that of Red5-GFP (Figure 6B), indicating that the deletion of the C-terminal region did not significantly affect the stability of the truncated protein.

Dilution analyses showed that the Red5ΔC-GFP strain grew considerably more slowly at 18, 26, 30 or 34°C than did the Red5-GFP strain; moreover, the Red5ΔC-GFP strain hardly grew at 37°C (Figure 6C). Consistent with this growth retardation, we found curved cells or cells with multisepta more often in Red5ΔC-GFP cells than in Red5-GFP cells grown at 30°C (Supplementary Figure S7A). With fluorescent microscopy, we observed Red5 foci in Red5ΔC-GFP and in Red5-GFP cells (Supplementary Figure S7B). Furthermore, iodine staining intensity and mating efficiency were lower in Red5ΔC-GFP cells than in Red5-GFP cells (Figures 6D and E), and the levels of DSR-containing meiotic mRNAs were higher in vegetative Red5ΔC-GFP cells than in

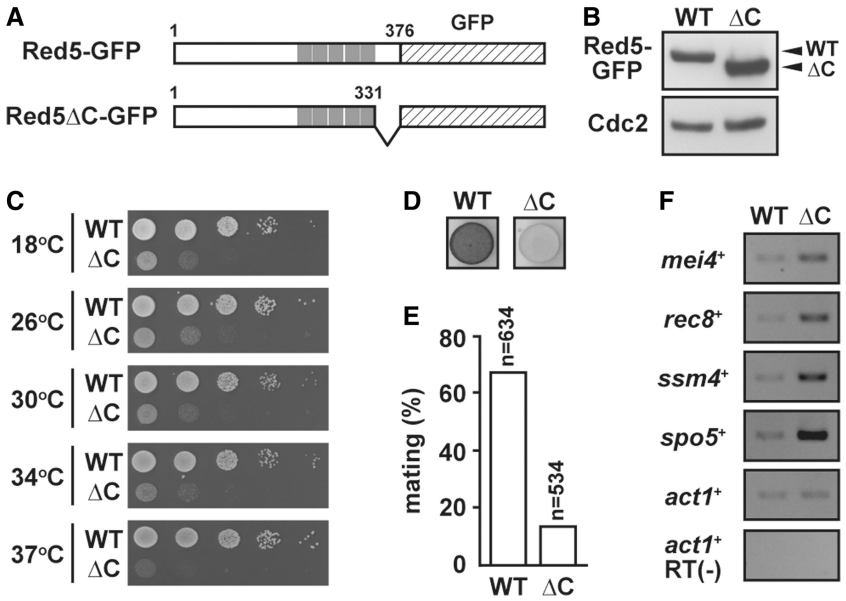

Figure 6. The C-terminal domain of Red5 is important for normal cell growth and meiotic mRNA elimination. (**A**) Schematic representation of two GFP-tagged Red5 constructs, a full-length (Red5-GFP) and a C-terminal truncated (Red5ΔC-GFP) construct. The zinc-finger domains are shown as gray boxes. Each version of the Red5 protein was expressed as a GFP fusion protein from the endogenous *red5*$^{+}$ locus. (**B**) Truncation of the C-terminal domain of Red5 does not affect the abundance of the protein. Protein extracts from Red5-GFP (WT) and Red5ΔC-GFP (ΔC) strains were examined on western blots probed with anti-GFP or anti-Cdc2 antibody. Cdc2 was monitored as the loading control. (**C**) Serial dilutions of Red5-GFP (WT) or Red5ΔC-GFP (ΔC) cultures were spotted onto YEA plates and then incubated at indicated temperatures. (**D**) Iodine staining was reduced in homothallic Red5ΔC-GFP cells when meiosis was induced. (**E**) Mating efficiency was reduced in Red5ΔC-GFP cells; 'n' indicates the number of cells counted for each strain. (**F**) The C-terminal truncation of Red5 led to the accumulation of meiotic mRNAs. Samples of total RNAs isolated from Red5-GFP and Red5ΔC-GFP strains were subjected to RT–PCR using primers specific for each of four meiotic mRNAs, *mei4*$^{+}$, *rec8*$^{+}$, *ssm4*$^{+}$ or *spo5*$^{+}$.

Red5-GFP cells (Figure 6F). These results further support the conclusion that Red5 is essential for selective decay of meiotic mRNAs, and they indicated that *red5* deficiency adversely affects the cell division cycle, and that the C-terminal domain of Red5, like the zinc-finger domains, is crucial for Red5 function.

Poly(A)$^{+}$ RNAs accumulate in the nucleolar region of *red5*-deficient cells

A previous study demonstrated that fly and human ZC3H3 proteins participate in mRNA export (32). Because the zinc-finger domains of Red5 showed homology to those of ZC3H3 proteins, we presumed that Red5 was also involved in mRNA export. To test this hypothesis, we performed RNA-FISH using oligo(dT) as a probe to determine whether poly(A)$^{+}$ RNA species accumulated in the nuclei of *red5-2* cells. At the permissive temperature (26°C), poly(A) signal was dispersed in both the nucleus and cytoplasm of wild-type, *red5*$^{+}$ and *red5-2* cells, and the signal seemed to be slightly enriched in the nucleus of *red5-2* cells (Figure 7). In contrast, at the restrictive temperature (37°C), the poly(A) signal was condensed and present in the non-chromatic regions of *red5-2* cells (Figure 7; Supplementary Figure S8A); in contrast, poly(A)$^{+}$ RNA signal was dispersed in wild-type and *red5*$^{+}$ cells at 37°C (Figure 7). This accumulation of poly(A)$^{+}$ RNA observed in *red5-2* started 15 min after temperature shift (Supplementary Figure S8B). As *red5-2* cells grew at 37°C (Figure 2C), the poly(A)$^{+}$ RNA that accumulated

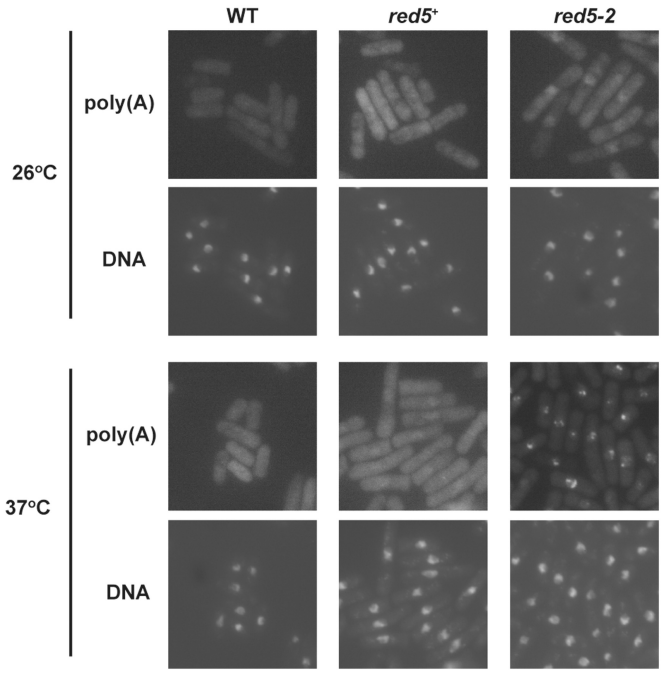

Figure 7. Poly(A)$^{+}$ RNA species accumulate as foci in the nucleoli of *red5-2* cells. Wild-type, *red5*$^{+}$–FLAG (*red5*$^{+}$) or *red5*^{I234Y}–FLAG (*red5-2*) cells were grown at 26°C and either maintained at 26°C (top two rows) or shifted to 37°C for 4 h (bottom two rows). The cells were fixed and analyzed by *in situ* hybridization with a biotin-labeled oligo(dT)$_{50}$ probe. Hybridized probes were detected by fluorescein isothiocyanate-conjugated avidin. The fluorescein isothiocyanate rows, indicated as poly(A), show the distribution of poly(A)$^{+}$ RNA in the respective cells. DNA in these cells was counterstained with 4′,6-Diamidino-2-phenylindole (DAPI).

in the nucleolus did not seem to reflect mRNA export deficiency.

Red5ΔC cells, unlike *red5-2* cells, showed a severe growth defect at all the temperatures (Figure 6C); therefore, we suspected that this growth retardation resulted from an mRNA export defect. We assessed poly(A)$^+$ RNA distribution in Red5ΔC cells and found that the signals from poly(A)$^+$ RNA species were intense in both the nuclear and nucleolar regions of Red5ΔC-GFP cells (Supplementary Figure S9), suggesting that mRNA export is apparently compromised in cells that lacked the Red5 C-terminal domain.

Red5 genetically interacts with various mRNA export factors and the nuclear poly(A)-binding protein Pab2

We examined genetic interactions to further characterize the relationship between Red5 and known factors involved in mRNA export. We examined genetic interactions between Red5 and five known mRNA export factors (Rae1, Dss1, Mex67, Ptr1 and Uap56), a plausible mRNA export factor Tho4 (SPBC106.12c, human THOC4 homolog) and Pab2 because each of these proteins contributes to different aspect of mRNA export (37,44,45). Cells carrying the *red5-2* allele and the *rae1-167*, *dss1*Δ, *mex67*Δ, *ptr1-1*, *tho4*Δ, *uap56-1* or *pab2*Δ mutation were viable, indicating that each of these pairwise combinations did not cause synthetic lethality. However, in serial dilution assays, we found synthetic growth defects in: *red5-2 rae1-167* (at 26 and 30°C), *red5-2 ptr1-1* (at 30°C, but only a weak growth defect), *red5-2 tho4*Δ (at 26, 30, 34, and 37°C), *red5-2 dss1*Δ (at 26, 30, and 34°C), *red5-2 pab2*Δ (at 18, 26, and 30°C), *red5-2 mex67*Δ (at 26, 30, and 34°C) and *red5-2 uap56-1* (at 37°C) cells (Supplementary Figure S10). We also observed phenotypic suppression in *red5-2 dss1*Δ (at 18°C) cells and in *red5-2 uap56-1* (at 18 and 26°C) cells (Supplementary Figure S10). Some of these results were also confirmed by measuring growth rates (Supplementary Figure S11).

We also examined whether Red5 overproduction rescued or inhibited cell growth of cells defective in mRNA export. Overexpression of the *red5*$^+$ gene under the control of the inducible *nmt1* (full-strength) or *nmt41* (medium-strength) promoter did not produce a noticeable phenotype in wild-type cells grown at any one of three temperatures (Supplementary Figure S12A and C). In addition, Red5 overexpression did not inhibit sporulation, whereas Mmi1 overexpression did (Supplementary Figure S12B). Furthermore, when *red5*$^+$ was overexpressed, we observed a noticeable reduction in growth in *dss1*Δ (at 26, 30 and 32°C), *mlo3*Δ (at 26, 30 and 32°C) and *ptr1-1* (at 32°C) strains, but not in the other strains (Supplementary Figure S12C). Red5 overexpression also had no effect on growth of *rae1-167*, *mex67*Δ or *uap56-1* strains, and Red5 did not act as a multi-copy suppressor of any of these mutations (Supplementary Figure S12C).

These data from RNA-FISH experiments and from assays of genetic interactions between Red5 and several mRNA export factors raised the possibility that Red5 physically bound to these mRNA export factors. We then performed a series of immunoprecipitation assays to examine whether Red5 interacted with Mex67, SPBC1105.07c (a homolog of *S. cerevisiae* Thp1, a component of TREX-2), Tho1 (SPCC31H12.03c, homologous to *S. cerevisiae* Tho1), Rae1, Mlo3 or Dss1. We found that Red5 did not coimmunoprecipitate markedly with any of these proteins (Supplementary Figure S13); however, we could not exclude the possibility that Red5 interacts with other mRNA export proteins. Taken together, these results indicated that Red5 genetically interacts with mRNA export factors and suggested the possibility that Red5 participates in mRNA export.

Rae1, Npp106 and Nup120, components of the nuclear pore complex, are involved in degradation of meiotic mRNAs

Poly(A)$^+$ RNA accumulation in *red5*-deficient cells and genetic interactions between Red5 and mRNA export factors prompted us to investigate whether mutations in mRNA export factors alleviated meiotic mRNA elimination. To test this idea, we examined the levels of DSR-containing meiotic mRNAs in *dss1*Δ, *mex67*Δ, *mlo3*Δ, *ptr1-1* or *rae1-167* cells. We found that four of DSR-containing meiotic mRNAs accumulated in *rae1-167* cells, but not in *dss1*Δ, *mex67*Δ, *mlo3*Δ or *ptr1-1* cells (Figure 8; Supplementary Figure S14A). We also carried out RT–PCR in the *mog1-1* strain (46) and in strains lacking one of five putative mRNA export factors—Sus1 (a subunit of SAGA complex and TREX-2), Tho1, Tho4, SPAC328.05 (homologous to *S. cerevisiae* Hrb1/Gbp2) or SPCC70.06 (a fission yeast homolog of *S. cerevisiae* Sac3); we did not observe any obvious increase in meiotic mRNAs in any of these strains (Supplementary Figures S14B and C). These

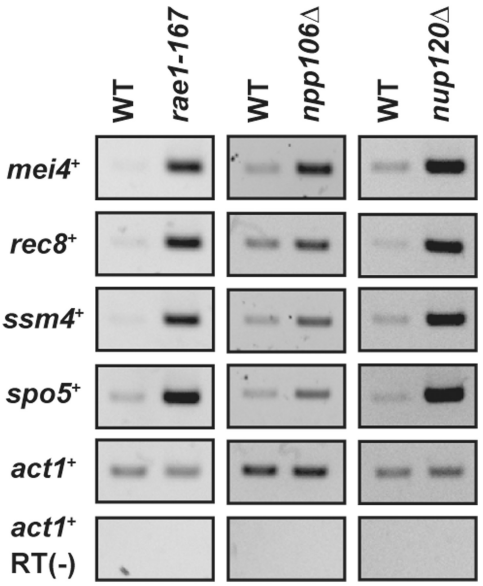

Figure 8. Rae1, Npp106 and Nup120, each components of the nuclear pore complex, are involved in meiotic mRNA elimination. Total RNA samples from wild-type, *rae1-167*, *npp106*Δ or *nup120*Δ cells were subjected to RT–PCR analyses to examine the levels of *mei4*$^+$, *rec8*$^+$, *ssm4*$^+$ and *spo5*$^+$ mRNAs.

results suggested that Rae1 has an additional role in meiotic mRNA decay, but they did not suggest that mRNA export factors are generally involved in meiotic mRNA decay.

Rae1 is homologous to *S. cerevisiae* Gle2, which is a component of the Nup82 subcomplex in the NPC, and Gle2 regulates poly(A)$^+$ mRNA export (47); therefore, it is likely that Rae1, like Gle2, is a subunit of the NPC. This speculation led us to suspect that other NPC components might participate in the selective removal of meiotic mRNAs. To test this hypothesis, we constructed strains that each lacked a gene encoding a different NPC protein, and then assessed the steady-state levels of meiotic mRNAs in these deletion strains. RT–PCR experiments demonstrated that the meiotic mRNA accumulation was elevated in vegetative *npp106*Δ and *nup120*Δ cells, but not in *nup60*Δ, *nup131*Δ, *nup132*Δ, *nup124*Δ, *seh1*Δ, *nup40*Δ or *pom152*Δ cells (Figure 8; Supplementary Figure S14B and D). These findings indicated that some, but not all, NPC proteins are essential for proper elimination of meiotic mRNAs in mitotic cells. Furthermore, we found that *red5-2 nup120*Δ cells, like *red5-2 rae1-167* cells, had a synthetic growth defect at 26 and 30°C (Supplementary Figure S15).

The NPCs have been shown to regulate gene expression at transcriptionally and post-transcriptionally (15,48). Therefore, we next examined whether these NPC components were involved in the downregulation of DSR-containing mRNAs. To address this issue, we first generated strains that carried a *ura4*$^+$-DSR marker (Figure 5A, top) and a *npp106*Δ or *rae1-167* mutation and tested whether *ura4*$^+$-DSR mRNA accumulated in each strain. As shown in Supplementary Figures S16A and B, *ura4*$^+$-DSR mRNA accumulated in *npp106*Δ and in *rae1-167* cells. Although Npp106 and Rae1 are each necessary for the suppression of meiotic mRNAs, a mutation in each protein only weakly affected this suppression when compared with deletion of the Red1 protein (Supplementary Figures S16A and B). These results suggested that these NPC components might not be critical players for meiotic mRNA degradation directed by DSR, but they might facilitate the degradation processes of DSR-dependent mRNA decay.

Red1 destabilizes meiotic mRNAs; consequently, we assumed that mutations in the NPC subunits also increased the stability of DSR-containing meiotic mRNAs. Therefore, we compared *npp106*Δ cells with wild-type cells with regard to the stability of the *ura4*$^+$-DSR transcript. We found that in wild-type cells, levels of *ura4*$^+$-DSR transcript decreased rapidly, within 10 min of the shutting down of the *nmt81* promoter with thiamine; in contrast, we found that in *npp106*Δ cells, levels of *ura4*$^+$-DSR mRNA did not change even 30 min after the shutting down of *ura4*$^+$-DSR transcription (Supplementary Figure S16C); these findings indicated that Npp106 promotes meiotic mRNA degradation by destabilizing DSR-containing RNAs. These results revealed an unexpected role for NPC subunits in the elimination of meiotic mRNAs in vegetative fission yeast.

DISCUSSION

In this study, we identified and characterized Red5, a previously uncharacterized zinc-finger protein that localizes to the nucleoplasm and forms discrete dots within the nucleus and nucleolus of fission yeast. We demonstrated that Red5 is required both for meiotic mRNA elimination in vegetative cells and for efficient mating. We also showed that *red5* deficiency results in the accumulation of poly(A)$^+$ RNA in the nucleus and nucleolus, and that Red5 genetically interacted with several mRNA export factors. Furthermore, we revealed that three components of NPCs are involved in the selective removal of meiotic mRNAs.

Red5 is a nuclear protein that carries C3H1-type Zn-finger domains. Zn-finger domains are often found in nucleic acid-binding proteins, and Red5 is involved in mRNA metabolism; therefore, it is plausible that the Zn-finger domains of Red5 also have RNA-binding activity. *Drosophila* ZC3H3 together with Swm, PABP2 and NXF1 associates with nuclear poly(A)$^+$ RNAs (32). Therefore, it is likely that ZC3H3 proteins could bind to polyadenylated RNA species, but we cannot exclude the possibilities that a protein or proteins interacting with ZC3H3 binds to poly(A)$^+$ RNAs and that the Zn-finger domains of ZC3H3 proteins act as a protein-interacting module. Biochemical analyses will reveal whether ZC3H3 proteins, including Red5, are indeed RNA-binding proteins.

Several proteins essential for selective meiotic mRNA decay were identified previously (6,9–11). These proteins are classified into two categories based on the length of the poly(A) tail of meiotic mRNAs in mutant or deletion strains; specifically, these proteins are classified as factors that are required for hyperadenylation of meiotic mRNAs (Mmi1, Red1 and Pla1) and as factors that are not required for the hyperadenylation (Rrp6 and Dis3). We found that a deficiency of Red5 function resulted in the accumulation of meiotic mRNAs that carry excessively elongated poly(A) tails; this observation suggested that Red5 should work at one or more steps after polyadenylation of meiotic mRNAs, such steps as recruitment of the nuclear exosome, mRNA degradation by the nuclear exosome or both. As Red5 interacted with Pab2, but not with Rrp6, we assumed that Red5, together with Pab2, may facilitate the recruitment of the nuclear exosome to target mRNAs. Recent findings demonstrated that in *S.cerevisiae*, Nab2 binds naked poly(A) tails that are not covered with Pab1 [a poly(A)-binding protein], and the Nab2 on these mRNAs is then replaced with Rrp6, thereby trimming elongated poly(A) tails (49). By analogy to these findings, we speculate that the following events occur: (i) Red5 binds to elongated parts of poly(A) tails directly or to the Pab2 coating such elongated poly(A) tails; (ii) Red5 attracts the nuclear exosome and is displaced by the nuclear exosome; and (iii) the nuclear exosome, once loaded onto meiotic mRNAs, degrades its target mRNAs. Another possibility is that Red5 mediates meiotic mRNA degradation by assisting the nuclear exosome, rather than by recruiting the exosome to target mRNAs. In this model, Pab2 binds to the elongated poly(A) tails of meiotic mRNAs, and this Pab2 association protects these meiotic mRNAs from non-specific

degradation by 3′–5′ exoribonucleases. When the nuclear exosome is recruited to target mRNAs probably by Mmi1/Red1/Pab2, Red5 somehow induces eviction of Pab2 from the poly(A) tails to facilitate meiotic mRNA decay by the exosome. Further analyses will be necessary to test each of these possibilities.

In humans and flies, RNAi-mediated knockdown of ZC3H3 proteins compromises mRNA export (32). We observed that poly(A)$^+$ RNAs were present in the nuclear and nucleolar regions of Red5ΔC cells, and that Red5 genetically interacts with several mRNA export factors; together these findings indicated that the role of ZC3H3 proteins in mRNA export is evolutionarily conserved in fission yeast, flies and humans. The Red5ΔC cells obviously displayed a severe growth retardation at all the temperatures we tested. As a defect in meiotic mRNA elimination does not always disrupt vegetative growth, dysfunction in mRNA export, rather than meiotic mRNA suppression, apparently undermined normal mitotic growth in Red5ΔC cells. Indeed, many mRNA export factors are essential for cell viability (e.g. Rae1, Uap56 and Ptr1) or required for normal vegetative growth (e.g. Dss1 and Mlo3) (37,44,50).

We also observed that poly(A)$^+$ RNA species accumulated in the nucleolar regions of *red5-2* cells. The poly(A)$^+$ RNA signals observed in *red5-2* cells at 37°C were clearly different from those observed in Red5ΔC cells or in mRNA export-deficient cells; the poly(A)$^+$ RNA signals were present in the nucleus of cells that were defective in mRNA export, such as *dss1*Δ and *mlo3*Δ cells (37). Therefore, it seemed that mRNA export was not affected in *red5-2* cells because *red5-2* cells, as well as wild-type cells, could grow at 37°C. A previous study showed that poly(A)$^+$ RNAs accumulate as foci in the nucleolus of *rrp6*Δ cells (51) in which meiotic mRNAs are stabilized and extensively polyadenylated (9,11). Therefore, we assume that poly(A)$^+$ RNA accumulation in the nucleoli of *red5-2* and *rrp6*Δ strains could be due, at least in part, to a deficiency in meiotic mRNA degradation. We still do not know the reason why poly(A)$^+$ RNAs were enriched in nucleoli. Given that the nuclear exosome works in the nucleoli to process and to degrade pre-rRNAs and pre-snoRNAs (52), the nucleolus may also be a place where meiotic mRNAs are degraded or a place for temporary storage of non-functional RNAs that are eventually degraded by the nuclear exosome.

We showed that Red5 functions in meiotic mRNA degradation and in general mRNA export. It is likely that these two functions are separable based on the three following observations: (i) mRNA export factors are not generally required for meiotic mRNA elimination; (ii) *red5-2* cells, like wild-type cells, grew at 37°C, even though meiotic mRNAs accumulated in the *red5-2* cells; and (iii) poly(A)$^+$ signals in the nucleus were overt only in a small fraction of *red1*Δ cells (N.W. and T.T., unpublished observation). However, we can not completely rule out the possibility that meiotic mRNA decay is somehow coupled with mRNA export processes, for example, the assembly of export-competent mRNPs.

Our analyses also demonstrated that three strains, each bearing a mutation or deletion in one component of the NPCs (*rae1-167*, *nup120*Δ or *npp106*Δ) showed elevated levels of meiotic mRNAs. This finding suggested that there may be connections between meiotic mRNA decay and the NPC. However, the mechanisms by which NPCs promote meiotic mRNA decay remain unknown. Rae1, Nup120 and Npp106 belong to different subcomplexes (Nup82, Nup107-160 or Nic96 subcomplex, respectively) of the NPC, and a mutation or deletion of these genes leads to a deficiency in mRNA export (45,53,54). As mRNA export did not seem to be generally required for meiotic mRNA elimination, there might be another common feature among these proteins. Notably, the RNA surveillance machinery, including the TRAMP complex and the nuclear exosome, apparently retain or degrade aberrant or non-functional RNA species in the vicinity of the NPCs (13,16). Moreover, human Nup98 regulates degradation of the p21^{CIP1} mRNA by the exosome, and Rrp6 is recruited to nascent transcripts and is then released from mRNPs near the NPCs in *Chironomus tentans* (48,55). These findings indicate that NPCs could provide a platform for mRNA degradation, and/or that the NPCs may regulate whether mRNPs are exported or degraded. The exact functions of the NPCs in meiotic mRNA degradation are currently under investigation, and it would be of great interest to test whether the role of NPC in mRNA decay is conserved among eukaryotes.

SUPPLEMENTARY DATA

Supplementary Data are available at NAR Online: Supplementary Tables 1–3 and Supplementary Figures 1–16.

ACKNOWLEDGEMENTS

The authors thank R. Dhar, V. Doye, K.Tatebayashi, M. Yamamoto and the National Bioresource Project (NBRP) of the Ministry of Education, Culture, Sports, Science and Technology (MEXT) for *S.pombe* strains. They also thank R. Tsien, Y. Watanabe and H. Ogawa for the mCherry-tagging vector and GFP cDNA; K. Inoue for valuable comments; Y. Mishima for both technical advice on RNase H digestion and helpful discussion; and T. Tsuboi for technical advice on northern blotting using the DIG system.

FUNDING

Japan Society for the Promotion of Science (JSPS) KAKENHI [22687013 to T.S.]; Ministry of Education, Culture, Sports, Science and Technology (MEXT) KAKENHI [23112716 to T.T.]; Precursory Research for Embryonic Science and Technology (PRESTO) of the Japan Science and Technology Agency (JST) (to T.S.); Nakajima Foundation (to T.S.); Sumitomo Foundation (to T.S.). Funding for open access charge: Japan Society for the Promotion of Science (JSPS) KAKENHI [22687013].

Conflict of interest statement. None declared.

REFERENCES

1. Gamsjaeger,R., Liew,C.K., Loughlin,F.E., Crossley,M. and Mackay,J.P. (2007) Sticky fingers: zinc-fingers as protein-recognition motifs. *Trends Biochem. Sci.*, **32**, 63–70.
2. Le Provost,F., Lillico,S., Passet,B., Young,R., Whitelaw,B. and Vilotte,J.L. (2010) Zinc finger nuclease technology heralds a new era in mammalian transgenesis. *Trends Biotechnol.*, **28**, 134–141.
3. Yamamoto,M. (1996) Regulation of meiosis in fission yeast. *Cell Struct. Funct.*, **21**, 431–436.
4. Mata,J., Lyne,R., Burns,G. and Bahler,J. (2002) The transcriptional program of meiosis and sporulation in fission yeast. *Nat. Genet.*, **32**, 143–147.
5. Chikashige,Y., Tsutsumi,C., Yamane,M., Okamasa,K., Haraguchi,T. and Hiraoka,Y. (2006) Meiotic proteins bqt1 and bqt2 tether telomeres to form the bouquet arrangement of chromosomes. *Cell*, **125**, 59–69.
6. Harigaya,Y., Tanaka,H., Yamanaka,S., Tanaka,K., Watanabe,Y., Tsutsumi,C., Chikashige,Y., Hiraoka,Y., Yamashita,A. and Yamamoto,M. (2006) Selective elimination of messenger RNA prevents an incidence of untimely meiosis. *Nature*, **442**, 45–50.
7. McPheeters,D.S., Cremona,N., Sunder,S., Chen,H.M., Averbeck,N., Leatherwood,J. and Wise,J.A. (2009) A complex gene regulatory mechanism that operates at the nexus of multiple RNA processing decisions. *Nat. Struct. Mol. Biol.*, **16**, 255–264.
8. Chen,H.M., Futcher,B. and Leatherwood,J. (2011) The fission yeast RNA binding protein Mmi1 regulates meiotic genes by controlling intron specific splicing and polyadenylation coupled RNA turnover. *PLoS One*, **6**, e26804.
9. Yamanaka,S., Yamashita,A., Harigaya,Y., Iwata,R. and Yamamoto,M. (2010) Importance of polyadenylation in the selective elimination of meiotic mRNAs in growing *S. pombe* cells. *EMBO J.*, **29**, 2173–2181.
10. St-Andre,O., Lemieux,C., Perreault,A., Lackner,D.H., Bahler,J. and Bachand,F. (2010) Negative regulation of meiotic gene expression by the nuclear poly(a)-binding protein in fission yeast. *J. Biol. Chem.*, **285**, 27859–27868.
11. Sugiyama,T. and Sugioka-Sugiyama,R. (2011) Red1 promotes the elimination of meiosis-specific mRNAs in vegetatively growing fission yeast. *EMBO J.*, **30**, 1027–1039.
12. Yamashita,A., Shichino,Y., Tanaka,H., Hiriart,E., Touat-Todeschini,L., Vavasseur,A., Ding,D.Q., Hiraoka,Y., Verdel,A. and Yamamoto,M. (2012) Hexanucleotide motifs mediate recruitment of the RNA elimination machinery to silent meiotic genes. *Open Biol.*, **2**, 120014.
13. Strambio-De-Castillia,C., Niepel,M. and Rout,M.P. (2010) The nuclear pore complex: bridging nuclear transport and gene regulation. *Nat. Rev. Mol. Cell Biol.*, **11**, 490–501.
14. Ryan,K.J. and Wente,S.R. (2000) The nuclear pore complex: a protein machine bridging the nucleus and cytoplasm. *Curr. Opin. Cell Biol.*, **12**, 361–371.
15. Dieppois,G. and Stutz,F. (2010) Connecting the transcription site to the nuclear pore: a multi-tether process that regulates gene expression. *J. Cell Sci.*, **123**, 1989–1999.
16. Fasken,M.B. and Corbett,A.H. (2009) Mechanisms of nuclear mRNA quality control. *RNA Biol.*, **6**, 237–241.
17. Dauer,W.T. and Worman,H.J. (2009) The nuclear envelope as a signaling node in development and disease. *Dev. Cell*, **17**, 626–638.
18. D'Angelo,M.A., Gomez-Cavazos,J.S., Mei,A., Lackner,D.H. and Hetzer,M.W. (2012) A change in nuclear pore complex composition regulates cell differentiation. *Dev. Cell*, **22**, 446–458.
19. Lupu,F., Alves,A., Anderson,K., Doye,V. and Lacy,E. (2008) Nuclear pore composition regulates neural stem/progenitor cell differentiation in the mouse embryo. *Dev. Cell*, **14**, 831–842.
20. Sugiyama,T., Sugioka-Sugiyama,R., Hada,K. and Niwa,R. (2012) Rhn1, a nuclear protein, is required for suppression of meiotic mRNAs in mitotically dividing fission yeast. *PLoS One*, **7**, e42962.
21. Moreno,S., Klar,A. and Nurse,P. (1991) Molecular genetic analysis of fission yeast *Schizosaccharomyces pombe*. *Methods Enzymol.*, **194**, 795–823.
22. Allshire,R.C., Javerzat,J.P., Redhead,N.J. and Cranston,G. (1994) Position effect variegation at fission yeast centromeres. *Cell*, **76**, 157–169.
23. Shaner,N.C., Campbell,R.E., Steinbach,P.A., Giepmans,B.N., Palmer,A.E. and Tsien,R.Y. (2004) Improved monomeric red, orange and yellow fluorescent proteins derived from *Discosoma sp.* red fluorescent protein. *Nat. Biotechnol.*, **22**, 1567–1572.
24. Ogawa,H., Yu,R.T., Haraguchi,T., Hiraoka,Y., Nakatani,Y., Morohashi,K. and Umesono,K. (2004) Nuclear structure-associated TIF2 recruits glucocorticoid receptor and its target DNA. *Biochem. Biophys. Res. Commun.*, **320**, 218–225.
25. Bahler,J., Wu,J.Q., Longtine,M.S., Shah,N.G., McKenzie,A. 3rd, Steever,A.B., Wach,A., Philippsen,P. and Pringle,J.R. (1998) Heterologous modules for efficient and versatile PCR-based gene targeting in *Schizosaccharomyces pombe*. *Yeast*, **14**, 943–951.
26. Williams,J.S., Hayashi,T., Yanagida,M. and Russell,P. (2009) Fission yeast Scm3 mediates stable assembly of Cnp1/CENP-A into centromeric chromatin. *Mol. Cell*, **33**, 287–298.
27. Sugioka-Sugiyama,R. and Sugiyama,T. (2011) Sde2: a novel nuclear protein essential for telomeric silencing and genomic stability in *Schizosaccharomyces pombe*. *Biochem. Biophys. Res. Commun.*, **406**, 444–448.
28. Sugiyama,T., Cam,H.P., Sugiyama,R., Noma,K., Zofall,M., Kobayashi,R. and Grewal,S.I. (2007) SHREC, an effector complex for heterochromatic transcriptional silencing. *Cell*, **128**, 491–504.
29. Azad,A.K., Tani,T., Shiki,N., Tsuneyoshi,S., Urushiyama,S. and Ohshima,Y. (1997) Isolation and molecular characterization of mRNA transport mutants in *Schizosaccharomyces pombe*. *Mol. Biol. Cell.*, **8**, 825–841.
30. Gulli,M.P., Girard,J.P., Zabetakis,D., Lapeyre,B., Melese,T. and Caizergues-Ferrer,M. (1995) gar2 is a nucleolar protein from *Schizosaccharomyces pombe* required for 18S rRNA and 40S ribosomal subunit accumulation. *Nucleic Acids Res.*, **23**, 1912–1918.
31. Mandel,C.R., Bai,Y. and Tong,L. (2008) Protein factors in pre-mRNA 3′-end processing. *Cell Mol. Life Sci.*, **65**, 1099–1122.
32. Hurt,J.A., Obar,R.A., Zhai,B., Farny,N.G., Gygi,S.P. and Silver,P.A. (2009) A conserved CCCH-type zinc finger protein regulates mRNA nuclear adenylation and export. *J. Cell. Biol.*, **185**, 265–277.
33. Kim,D.U., Hayles,J., Kim,D., Wood,V., Park,H.O., Won,M., Yoo,H.S., Duhig,T., Nam,M., Palmer,G. *et al.* (2010) Analysis of a genome-wide set of gene deletions in the fission yeast *Schizosaccharomyces pombe*. *Nat. Biotechnol.*, **28**, 617–623.
34. Chinen,M., Morita,M., Fukumura,K. and Tani,T. (2010) Involvement of the spliceosomal U4 small nuclear RNA in heterochromatic gene silencing at fission yeast centromeres. *J. Biol. Chem.*, **285**, 5630–5638.
35. Goldar,M.M., Jeong,H.T., Tanaka,K., Matsuda,H. and Kawamukai,M. (2005) Moc3, a novel Zn finger type protein involved in sexual development, ascus formation, and stress response of *Schizosaccharomyces pombe*. *Curr. Genet.*, **48**, 345–355.
36. Wang,S.W., Asakawa,K., Win,T.Z., Toda,T. and Norbury,C.J. (2005) Inactivation of the pre-mRNA cleavage and polyadenylation factor Pfs2 in fission yeast causes lethal cell cycle defects. *Mol. Cell Biol.*, **25**, 2288–2296.
37. Thakurta,A.G., Gopal,G., Yoon,J.H., Kozak,L. and Dhar,R. (2005) Homolog of BRCA2-interacting Dss1p and Uap56p link Mlo3p and Rae1p for mRNA export in fission yeast. *EMBO J.*, **24**, 2512–2523.
38. Selvanathan,S.P., Thakurta,A.G., Dhakshnamoorthy,J., Zhou,M., Veenstra,T.D. and Dhar,R. (2010) *Schizosaccharomyces pombe* Dss1p is a DNA damage checkpoint protein that recruits Rad24p, Cdc25p, and Rae1p to DNA double-strand breaks. *J. Biol. Chem.*, **285**, 14122–14133.
39. Okuzaki,D., Kasama,T., Hirata,A., Ohtaka,A., Kakegawa,R. and Nojima,H. (2010) Spo5 phosphorylation is essential for its own timely degradation and for successful meiosis in *Schizosaccharomyces pombe*. *Cell Cycle*, **9**, 3751–3760.
40. Amorim,M.J., Cotobal,C., Duncan,C. and Mata,J. (2010) Global coordination of transcriptional control and mRNA decay during cellular differentiation. *Mol. Syst. Biol.*, **6**, 380.

41. Watanabe,Y. and Yamamoto,M. (1994) *S. pombe* mei2+ encodes an RNA-binding protein essential for premeiotic DNA synthesis and meiosis I, which cooperates with a novel RNA species meiRNA. *Cell*, **78**, 487–498.
42. Yamamoto,M. (2010) The selective elimination of messenger RNA underlies the mitosis-meiosis switch in fission yeast. *Proc. Jpn. Acad. Ser. B Phys. Biol. Sci.*, **86**, 788–797.
43. Yamamoto,A. and Hiraoka,Y. (2003) Monopolar spindle attachment of sister chromatids is ensured by two distinct mechanisms at the first meiotic division in fission yeast. *EMBO J.*, **22**, 2284–2296.
44. Andoh,T., Azad,A.K., Shigematsu,A., Ohshima,Y. and Tani,T. (2004) The fission yeast ptr1+ gene involved in nuclear mRNA export encodes a putative ubiquitin ligase. *Biochem. Biophys. Res. Commun.*, **317**, 1138–1143.
45. Brown,J.A., Bharathi,A., Ghosh,A., Whalen,W., Fitzgerald,E. and Dhar,R. (1995) A mutation in the *Schizosaccharomyces pombe* rae1 gene causes defects in poly(A)+ RNA export and in the cytoskeleton. *J. Biol. Chem.*, **270**, 7411–7419.
46. Tatebayashi,K., Tani,T. and Ikeda,H. (2001) Fission yeast Mog1p homologue, which interacts with the small GTPase Ran, is required for mitosis-to-interphase transition and poly(A)(+) RNA metabolism. *Genetics*, **157**, 1513–1522.
47. Murphy,R., Watkins,J.L. and Wente,S.R. (1996) GLE2, a *Saccharomyces cerevisiae* homologue of the *Schizosaccharomyces pombe* export factor RAE1, is required for nuclear pore complex structure and function. *Mol. Biol. Cell*, **7**, 1921–1937.
48. Singer,S., Zhao,R., Barsotti,A.M., Ouwehand,A., Fazollahi,M., Coutavas,E., Breuhahn,K., Neumann,O., Longerich,T., Pusterla,T. *et al.* (2012) Nuclear pore component Nup98 is a potential tumor suppressor and regulates posttranscriptional expression of select p53 target genes. *Mol. Cell*, **48**, 799–810.
49. Schmid,M., Poulsen,M.B., Olszewski,P., Pelechano,V., Saguez,C., Gupta,I., Steinmetz,L.M., Moore,C. and Jensen,T.H. (2012) Rrp6p controls mRNA poly(A) tail length and its decoration with poly(A) binding proteins. *Mol. Cell*, **47**, 267–280.
50. Mannen,T., Andoh,T. and Tani,T. (2008) Dss1 associating with the proteasome functions in selective nuclear mRNA export in yeast. *Biochem. Biophys. Res. Commun.*, **365**, 664–671.
51. Zhang,K., Fischer,T., Porter,R.L., Dhakshnamoorthy,J., Zofall,M., Zhou,M., Veenstra,T. and Grewal,S.I. (2011) Clr4/Suv39 and RNA quality control factors cooperate to trigger RNAi and suppress antisense RNA. *Science*, **331**, 1624–1627.
52. Vanacova,S. and Stefl,R. (2007) The exosome and RNA quality control in the nucleus. *EMBO Rep.*, **8**, 651–657.
53. Bai,S.W., Rouquette,J., Umeda,M., Faigle,W., Loew,D., Sazer,S. and Doye,V. (2004) The fission yeast Nup107-120 complex functionally interacts with the small GTPase Ran/Spi1 and is required for mRNA export, nuclear pore distribution, and proper cell division. *Mol. Cell Biol.*, **24**, 6379–6392.
54. Yoon,J.H., Whalen,W.A., Bharathi,A., Shen,R. and Dhar,R. (1997) Npp106p, a *Schizosaccharomyces pombe* nucleoporin similar to *Saccharomyces cerevisiae* Nic96p, functionally interacts with Rae1p in mRNA export. *Mol. Cell Biol.*, **17**, 7047–7060.
55. Hessle,V., von Euler,A., Gonzalez de Valdivia,E. and Visa,N. (2012) Rrp6 is recruited to transcribed genes and accompanies the spliced mRNA to the nuclear pore. *RNA*, **18**, 1466–1474.